Chemical Science

ROYAL SOCIETY OF CHEMISTRY

EDGE ARTICLE

View Article Online
View Journal | View Issue

Check for updates

Cite this: *Chem. Sci.*, 2025, **16**, 1155

All publication charges for this article have been paid for by the Royal Society of Chemistry

Open Access Article. Published on 03 2024. Downloaded on 12.5.2026 15:04:04. This article is licensed under a Creative Commons Attribution-NonCommercial 3.0 Unported Licence.

Sub-*m*-benziporphyrin: a subcarbaporphyrinoid and its B^{III} complex with an unprecedented planar tridentate 14π-aromatic network†

Le Liu,[a] Shuangji Song,[a] Jiyeon Lee,[b] Yutao Rao,[a] Ling Xu,[a] Mingbo Zhou,[a] Bangshao Yin,[a] Juwon Oh,[c] Jiwon Kim, *[b] Atsuhiro Osuka*[a] and Jianxin Song *[a]

Received 23rd October 2024
Accepted 2nd December 2024

DOI: 10.1039/d4sc07199a

rsc.li/chemical-science

Sub-*m*-benziporphyrins were synthesized by Pd-catalyzed cross-coupling of α,α′-diboryl-*m*-benzitripyrrane with 9,10-bis(1,1-dibromomethylenyl)anthracene. Reaction of sub-*m*-benziporphyrin with $PhBCl_2$ and triethylamine gave its B-phenyl complex as a tetracoordinate nonaromatic B^{III} complex. In contrast, the reaction with BBr_3 and triethylamine furnished a neutral B^{III} porphyrinoid with a planar and triangular coordination as the first example, in which the *m*-phenylene unit was partially reduced, allowing for the global 14π-aromatic circuit. This aromatic B^{III} complex is stable and inert towards nucleophiles such as pyridine, 4-dimethylaminopyridine, and fluoride anions but undergoes an oxygen-insertion reaction upon refluxing in the air. In addition, this B^{III} complex displays structured vibronic Q-bands, slow S_1-state decay, and fluorescence ($\Phi_F = 0.30$ and $\tau_F = 9.7$ ns), in line with its aromatic nature, while the nonaromatic B^{III} complexes show ill-defined absorption spectra and very fast S_1-state decays.

Introduction

The chemistry of B^{III} subporphyrins started with our first synthesis in 2006.[1] Since then, their appealing attributes have been extensively explored,[2–6] which include 14π-aromatic electronic circuit, large substituent effects of *meso*-aryl substituents,[7–9] and relatively strong S_2-fluorescence;[10] they are used in the synthesis of stable subporphyrin B-hydrides,[11] and as effective dyes in dye-sensitized solar cells, achieving over 10% efficiency in the first trial.[12] Importantly, B^{III} porphyrinoids so far explored have all four-coordinated structures, as seen for B^{III} subporphyrins,[1] B^{III} subphthalocyanines,[6] and other B^{III} porphyrinoids.[13,14] The typical structure of B^{III} subporphyrins is a bowl shape tetracoordinated to three pyrrolic nitrogen atoms and an axial ligand. There has been no example of neutral tridentate B^{III} complexes of porphyrinoids, while cationic tridentate B^{III} complexes were reported as borenium cations.[15,16]

On the other hand, sterically non-hindered triarylboranes are usually air and moisture sensitive[17] but "structurally constrained" triarylboranes are known as exceptionally stable species,[18–22] in which an enforced planar geometry endows a particular stability. This strategy has been extended to directly diphenylborane-fused porphyrins.[23] In this paper, we report the first example of a neutral tridentate B^{III} subporphyrinoid.

Considering the rich and important chemistry of core-modified porphyrins,[24–31] the exploration of core-modified B^{III} subporphyrins is highly desirable but such compounds have been rare so far. As a core-modified variant, Latos-Grażyński *et al.* reported sub-*m*-pyriporphyrin as the first core-modified subporphyrin, which is a stable free base with a non-aromatic character.[32]

In 2022, we reported the first synthesis of subporphyrin free bases **3** and **4** by the Suzuki–Miyaura cross coupling reaction between α,α′-diborylated tripyrrane **1** and 9,10-bis(1,1-dibromomethylenyl)anthracene **2** (Scheme 1), where the use of **2** was crucial.[33] This synthetic success encouraged us to consider that a similar cross coupling reaction of α,α′-diboryl-*m*-benzitripyrrane **5** with **2** may allow for the synthesis of sub-*m*-benziporphyrins as an example of subcarbaporphyrinoid. Carbaporphyrins are porphyrin analogues, in which one or more of the pyrrolic nitrogen atoms are replaced by carbon atoms.[31,34] These porphyrinoids exhibit a characteristic coordination behavior to stabilize higher oxidation states of transition metals owing to the inner carbon atom.[31,34] Carbaporphyrins include N-confused porphyrins (NCP),[34,35] benziporphyrins,[24–27,30,31] and

[a]*Key Laboratory of Chemical Biology and Traditional Chinese Medicine, Ministry of Educational of China, Key Laboratory of the Assembly and Application of Organic Functional Molecules of Hunan Province, College of Chemistry and Chemical Engineering, Hunan Normal University, Changsha 410081, China. E-mail: jxsong@hunnu.edu.cn; atsuhiroosuka@hunnu.edu.cn*

[b]*School of Integrated Technology, College of Computing, Integrated Science and Engineering Division, Underwood International College, Integrative Biotechnology and Translational Medicine, Graduate School, Yonsei University, Incheon 21983, Korea. E-mail: jiwon.kim@yonsei.ac.kr*

[c]*Department of Chemistry, Soonchunhyang University, Asan 31538, Korea*

† Electronic supplementary information (ESI) available. CCDC 2379624 (for **6**), 2379625 (for **8**), 2379626 (for **9**), 2379627 (for **10**), 2379628 (for **11**), and 2379629 (for **12**). For ESI and crystallographic data in CIF or other electronic format see DOI: https://doi.org/10.1039/d4sc07199a

© 2025 The Author(s). Published by the Royal Society of Chemistry

Open Access Article. Published on 03 2024. Downloaded on 12.5.2026 15:04:04.
This article is licensed under a Creative Commons Attribution-NonCommercial 3.0 Unported Licence.

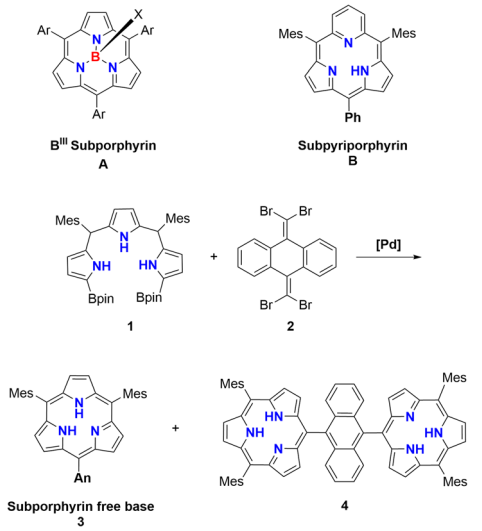

Scheme 1 Synthesis of subporphyrin free bases.

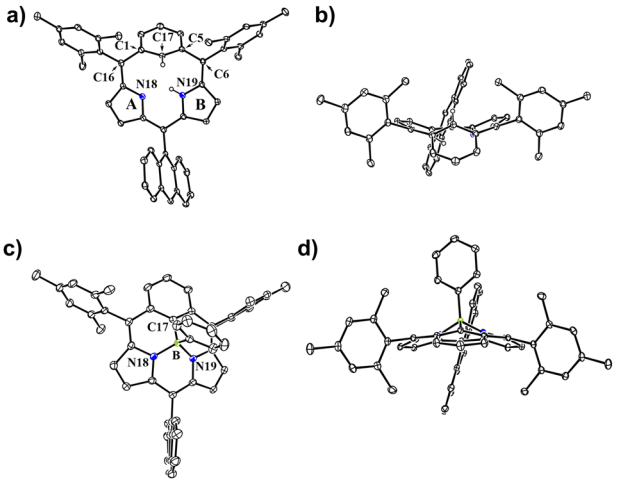

Fig. 1 X-ray single-crystal structures of **6** and **8**. (a) Top view of **6**; (b) side view of **6**; (c) top view of **8**; (d) side view of **8**. The thermal ellipsoids are scaled to the 30% probability level. All hydrogen atoms except those connected to N atoms are omitted for clarity.

expanded carbaporphyrins[36–38] but subcarbaporphyrinoids have been unprecedented.[39]

Results and discussion

Suzuki–Miyaura cross coupling of **5** with **2** (SPhos Pd G_2, K_3PO_4, toluene/DMF, 115 °C, 48 h) and subsequent oxidation with 2,3-dichloro-5,6-dicyano-1,4-benzoquinone (DDQ) gave a complicated mixture, from which sub-*m*-benziporphyrin **6** (6%) and anthracene-bridged sub-*m*-benziporphyrin dimer **7** (3%) were isolated (Scheme 2). The structure of **6** has been revealed by single-crystal X-ray diffraction analysis to be nonplanar, being roughly similar to that of the subporphyrin free base[33] (Fig. 1a and b). The amino-pyrrole B and the *m*-phenylene unit C are directed to the opposite side, probably to avoid the steric congestion between the inner NH and CH. The nonplanar structure of **6** is indicated by relatively large dihedral angles: 41.97(6)° between the pyrroles A and B; 40.43(7)° for the pyrrole B and the *m*-phenylene C; and 39.16(16)° for the *m*-phenylene and the pyrrole A. The C(1)–C(16) and C(5)–C(6) bond distances are 1.499(3) and 1.497(3) Å, underscoring that the *m*-phenylene unit is not conjugated with the dipyrrin unit. The ^{1}H NMR spectrum of **6** shows a singlet at 19.54 ppm due to the inner pyrrolic N–proton, a pair of doublets at 6.67 ppm and 6.18 ppm due to the pyrrolic β-protons and a broad signal at 6.65 ppm due to the inner proton of the *m*-phenylene unit. The NICS value[40] in the center of the optimized structure **6** has been calculated to be 1.15 ppm (see ESI Fig. S34†), being consistent with the assignment as a nonaromatic species. High-resolution MALDI-TOF mass spectroscopy detected the parent ion peak of **7** at m/z = 1134.5505 (calcd for $(C_{84}H_{70}N_4)^+$ = 1134.5595([M]$^+$). In the ^{1}H NMR spectrum of **7**, two singlets are observed for the inner NH protons and the inner CH protons of the *m*-phenylene unit, reflecting the presence of two tautomers with respect to the positions of the inner NH protons. We tried the coupling reactions with other geminal dibromides such as 1,1-dibromro-2,2-diphenylethene but failed to get sub-*m*-benziporphyrin. These results underscore the importance of dibromide **2**, similar to the synthesis of subporphyrin free bases.[33]

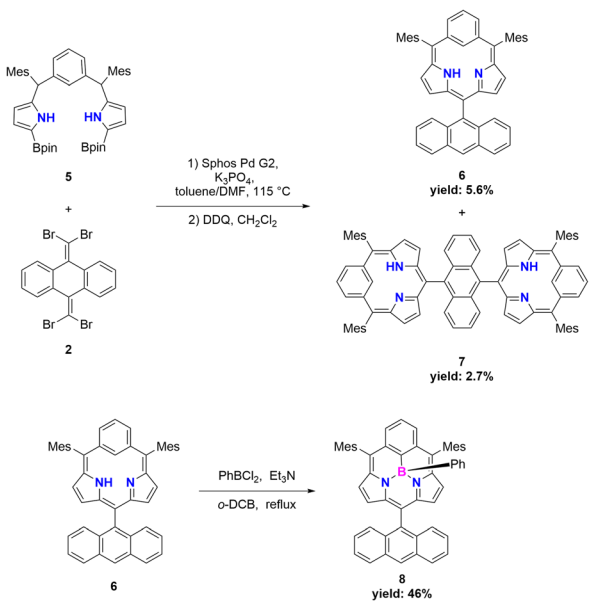

Scheme 2 Synthesis of **6**, **7**, and **8**. Mes = 2,4,6-trimethylphenyl, Bpin = pinacolatoboryl, DDQ = 2,3-dicyano-5,6-dichlorobenzoquinone.

The boron-coordinating ability of **6** has been examined by the reaction with freshly distilled $PhBCl_2$ in a boiling mixture of *o*-dichlorobenzene and triethylamine (TEA), which gave B-phenyl B[III] sub-*m*-benziporphyrin **8** in 46% yield (Scheme 2). The structure of **8** has been confirmed by X-ray analysis to be a tetra-coordinate bowl-shape similar to those of B[III] subporphyrins[1] (Fig. 1c and d). The bowl-depth, defined by the distance between the boron atom and the mean plane of the four peripheral β-carbons and two carbons at the positions 3

© 2025 The Author(s). Published by the Royal Society of Chemistry

Open Access Article. Published on 03 2024. Downloaded on 12.5.2026 15:04:04.
This article is licensed under a Creative Commons Attribution-NonCommercial 3.0 Unported Licence.

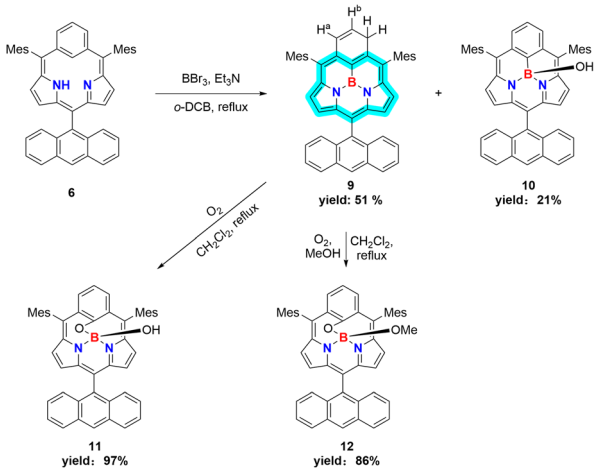

Scheme 3 Synthesis of B^{III} sub-*m*-benziporphyrins **9**, **10**, **11**, and **12**.

and 5 of the benzene, is 1.321(17) Å, which is distinctly shorter than that (*ca.* 1.42 Å) of the typical B^{III} subporphyrins. The bond lengths of the B–N(18), B–N(19), and B–C(17) are 1.515(17) Å, 1.523(17) Å, and 1.575(19) Å, respectively. The B–C(17) bond length is distinctly longer than those (1.500(5) Å) of the B–N in the typical B^{III} subporphyrins. The ^{1}H NMR spectrum of **8** shows a pair of doublets at 6.64 ppm and 6.10 ppm due to the pyrrolic β-protons, indicating the nonaromatic character of **8**.

In the next step, we examined the reaction of **6** with BBr_3 in a boiling mixture of *o*-dichlorobenzene and TEA, which afforded B^{III} sub-*m*-benziporphyrin **9** (51%) and B-hydroxy sub-*m*-benziporphyrin **10** (21%) (Scheme 3). The formation of **9** was unexpected but interesting. The structure of **9** has been unambiguously revealed by X-ray analysis to be a planar triangle coordination structure without an axial group (Fig. 3a and b), entirely different from the bowl-shaped structures of **8** and the usual B^{III} subporphyrins. Mean-plane deviation (MPD) of **9** is very small (0.15 Å). The bond lengths of the B–N(18), B–N(19), and B–C(17) are 1.396(5) Å, 1.385(5) Å, and 1.474(5) Å, respectively, being noticeably shorter than those of the complex **8**. It is worth noting that **9** is *the first example of tri-coordinated planar B^{III}porphyrinoid*. Importantly, the *m*-phenylene unit is reduced to an *exo*-methylene cyclohexadiene unit, allowing for the global 14π-aromatic electronic network as indicated in blue (Scheme 3). In line with this 14π-aromatic circuit, the ^{1}H NMR spectrum of **9** displays signals due to the β-protons at 7.58, 7.56, 7.45, and 7.41 ppm apparently in a downfield region, indicating a diatropic ring current, and signals due to the vinylene protons at 6.67 and 6.25 ppm (Fig. 2). The NICS values in the inner region of the optimized structure are calculated to be −9.58 ∼ −11.64 ppm (see ESI Fig. S36†). The structure of **10** has been confirmed by X-ray analysis to be analogous to that of **8** as shown in Fig. 3c and d. We also examined the reaction of **6** with only BBr_3, which gave **10** almost quantitatively.

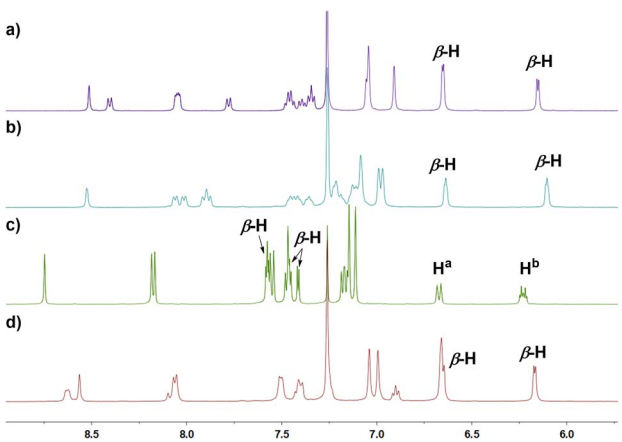

Fig. 2 ^{1}H NMR spectra of (a) **6** in $CDCl_3$ at 293 K; (b) **8** in $CDCl_3$ at 293 K; (c) **9** in $CDCl_3$ at 293 K; (d) **11** in $CDCl_3$ at 293 K.

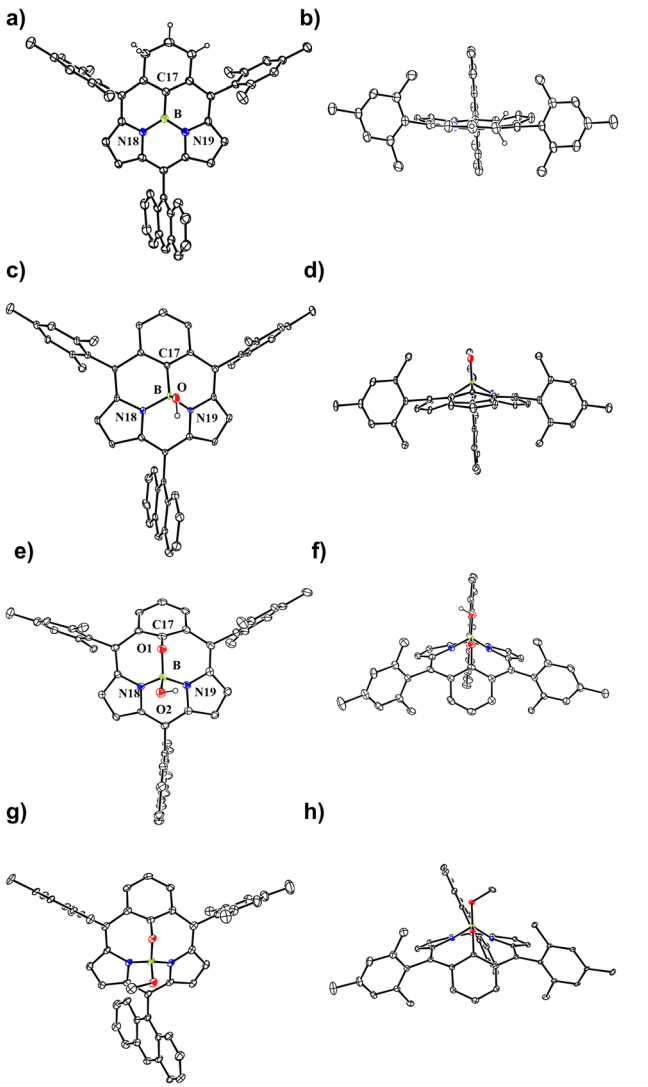

Fig. 3 X-ray single-crystal structures of **9**, **10**, **11**, and **12**. (a) Top view of **9**; (b) side view of **9**; (c) top view of **10**; (d) side view of **10**. (e) Top view of **11**; (f) side view of **11**; (g) top view of **12**; (h) side view of **12**. The thermal ellipsoids are scaled to the 30% probability level. All hydrogen atoms except those connected to N and O atoms are omitted for clarity.

Open Access Article. Published on 03 2024. Downloaded on 12.5.2026 15:04:04. This article is licensed under a Creative Commons Attribution-NonCommercial 3.0 Unported Licence.

In addition, it is worth noting that **9** exhibits high chemical stability under ambient conditions. Interestingly, **9** does not react with nucleophiles such as pyridine, 4-dimethylaminopyridine, or tetrabutylammonium fluoride as a rare case of neutral B^{III} compounds. On the other hand, refluxing of a solution of **9** in CH_2Cl_2 in the air for 48 h gave oxygen-inserted product **11** almost quantitatively. The structure of **11** has been revealed by X-ray analysis to have an inserted oxygen atom between the boron and ipso-carbon of the *m*-phenylene unit and the central B^{III} has an axial hydroxy group (Fig. 3e and f). The bond lengths are 1.366(4) Å for C(17)–O(1), 1.548(5) Å for B–N(18), 1.551(5) Å for B–N(19), 1.429(5) Å for B–O(1), and 1.416(5) Å for B–O(2). The extremely short C(17)–O(1) bond is arising from the small cavity. The ^{1}H NMR spectrum of **11** shows a pair of doublets at 6.64 ppm and 6.17 ppm due to the pyrrolic β-protons, indicating the nonaromatic character. The oxygenation of **9** was conducted in the presence of methanol to give **12**, which carries an axial methoxy group as evinced by X-ray analysis. The bond length of C(17)–O(1) is also short (1.358(4) Å).

The UV-vis absorption spectra of **6**, **7**, **8**, **9**, **11**, and **12** are shown in Fig. 4. Monomer **6** shows broad bands at 384 and 673 nm and dimer **7** shows nearly an identical spectrum with twice the extinction coefficients, indicating negligible electronic interaction between the two sub-benziporphyrin units. Compared to **6**, **8** exhibits a similar band at 388 nm and a red-shifted and broad band at 803 nm. In contrast, the absorption spectrum of **9** is quite different, displaying sharp bands at 335 and 356 nm and sharp vibronic-structured bands at 511 and 546 nm. Moreover, **9** emits fluorescence at 559 nm with Φ_F = 0.30 and τ_F = 9.7 ns (see ESI Fig. S38 and S46†). These contrasting optical properties of **9** can be attributed to its distinct aromatic nature. The electron density delocalized bond (EDDB) analysis visualizes nonaromatic cyclic π-conjugation for **6** and **8** (see ESI Fig. S40 and S41†).[41,42] On the basis of these electronic structures, the broad lowest absorption bands of **6** and **8** are ascribed primarily to the HOMO–LUMO transitions (see ESI Fig. S43 and S44†). On the other hand, the cyclic delocalization feature is shown for **9** by EDDB (see ESI Fig. S42†), indicating that its vibronic-structured absorption bands and intense fluorescence come from the aromatic nature.[43–45] In this regard, the similar absorption spectral features of **11** and **12** to **6** are consistent with their nonaromatic nature.

We further measured transient absorption (TA) spectra of **6**, **8**, and **9** to investigate their excited-state dynamics (Fig. 5). The TA spectra of nonaromatic **6** and **8** rapidly decayed within tens of picoseconds. This is consistent with their nonaromatic nature, since such species show fast non-radiative decays. In sharp contrast, substantially long-live TA spectra were observed for **9**, which decayed double exponentially with time constants of 10.7 ns and longer than 5 μs. Here, the faster decay is well matched with its fluorescence lifetime, being assigned as the S_1 state decay. The long-lived TA signal can be assigned as the T_1 state, since it is considered that the long-lived S_1-state may have an ample time to undergo intersystem crossing to give the T_1 state.

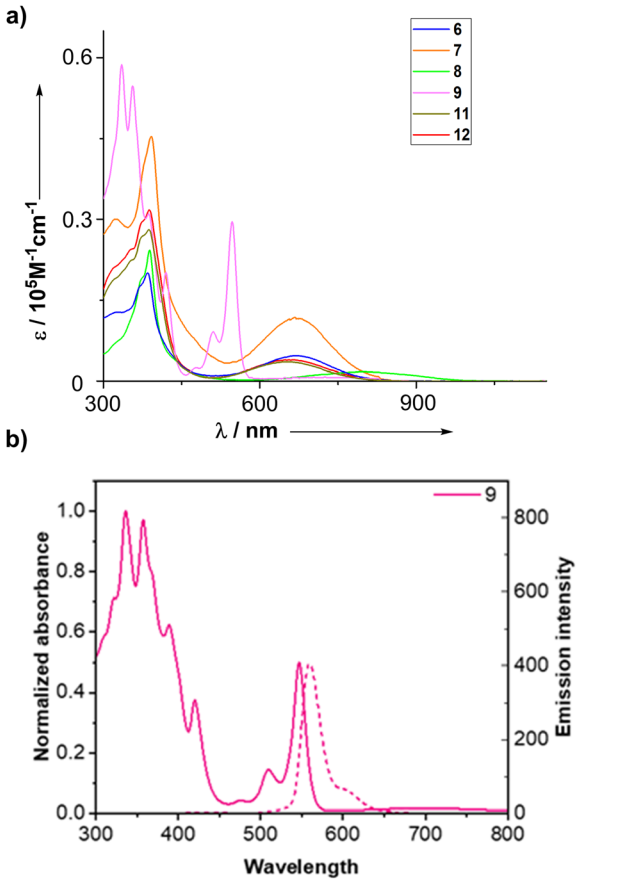

Fig. 4 (a) UV absorption spectra of **6**, **7**, **8**, **9**, **11**, and **12**. (b) UV-vis and fluorescence spectra of **9** with solid and dotted lines, respectively.

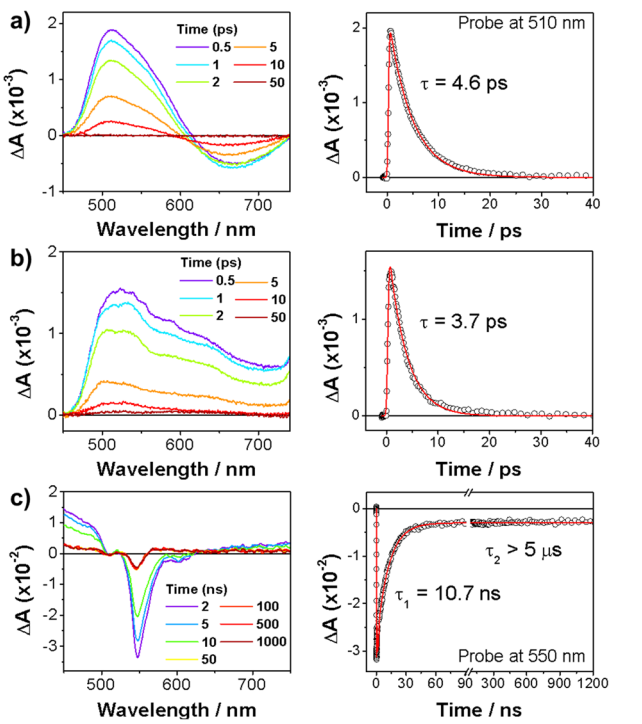

Fig. 5 TA spectra (left) and decay profiles (right) of (a) **6**, (b) **8**, and (c) **9** in Ar-bubbled toluene with photoexcitation at 400 nm.

© 2025 The Author(s). Published by the Royal Society of Chemistry

Open Access Article. Published on 03 2024. Downloaded on 12.5.2026 15:04:04. This article is licensed under a Creative Commons Attribution-NonCommercial 3.0 Unported Licence.

Conclusions

In summary, sub-*m*-benziporphyrins were synthesized by the cross-coupling of α,α'-diboryl-*m*-benzitripyrrane with 9,10-bis(1,1-dibromomethylenyl)anthracene as an example of sub-carbaporphyrinoid. The sub-*m*-benziporphyrin was converted to a B-phenyl B^{III} complex upon treatment with $PhBCl_2$ and TEA. These sub-*m*-benziporphyrins and their B^{III} complexes are nonaromatic owing to the cross-conjugated networks as evinced by their ^1H NMR spectra and absorption spectra. In contrast, the reaction of sub-*m*-benziporphyrin with BBr_3 and TEA gave a B^{III} complex that showed a planar and tridentate coordination of B^{III} as the first example of neutral B^{III} porphyrinoid. In addition, the *m*-phenylene unit is concurrently reduced to an *exo*-methylene cyclohexadiene unit, which allows the global 14π-aromatic circuit. The aromatic B^{III} complex is stable towards nucleophiles but undergoes oxygen-insertion reaction upon treatment with the atmospheric oxygen at reflux in CH_2Cl_2. While the nonaromatic B^{III} complexes **6** and **8** show ill-defined absorption spectra and very fast S_1-state decays, the aromatic B^{III} complex **9** displays structured Q-bands, slow S_1-state decay, and fluorescence. The exploration of novel ring-contracted carbaporphyrins with novel reactivities and properties is ongoing in our laboratory.

Data availability

The X-ray crystallographic coordinates for structures reported in this study have been deposited at the Cambridge Crystallographic Data Centre (CCDC), under deposition numbers 2379624 (for **6**), 2379625 (for **8**), 2379626 (for **9**), 2379627 (for **10**), 2379628 (for **11**), and 2379629 (for **12**). All experimental data and detailed experimental procedures are available in the ESI.†

Author contributions

J. Song designed and conducted the project. L. Liu, S. Song, J. Lee, J. Oh, and Y. Rao performed the synthesis and characterization, and measured the optical and electrochemical properties. L. Xu, M. Zhou, and B. Yin performed X-ray diffraction analysis and DFT calculations. J. Kim, A. Osuka, and J. Song prepared the manuscript.

Conflicts of interest

There are no conflicts to declare.

Acknowledgements

The work is supported by the National Natural Science Foundation of China (grant no. 22471070, 22471071, 22071052, 22201072, and 22271091), Science and Technology Planning Project of Hunan Province (2018TP1017), and Science and Technology Innovation Program of Hunan Province (2021RC4059). The work is also supported by the NRF funded by the Korea Government (MSIT) (no. RS-2023-00240624, RS-2024-00343229, and 2021R1A6A1A03039503).

Notes and references

1 Y. Inokuma, J.-H. Kwon, T. K. Ahn, M.-C. Yoo, D. Kim and A. Osuka, *Angew. Chem., Int. Ed.*, 2006, **45**, 961.
2 Y. Inokuma and A. Osuka, *Dalton Trans.*, 2008, 2517.
3 A. Osuka, E. Tsurumaki and T. Tanaka, *Bull. Chem. Soc. Jpn.*, 2011, **84**, 679.
4 C. G. Claessens, D. González Rodríguez, M. S. Rodríguez-Morgade, A. Medina and T. Torres, *Chem. Rev.*, 2014, **114**, 2192.
5 S. Shimizu, *Chem. Rev.*, 2017, **117**, 2730.
6 G. Lavarda, J. Labella, M. V. Martínez-Díaz, M. S. Rodríguez-Morgade, A. Osuka and T. Torres, *Chem. Soc. Rev.*, 2022, **51**, 9482.
7 Y. Inokuma, Z. S. Yoon, D. Kim and A. Osuka, *J. Am. Chem. Soc.*, 2007, **129**, 4747.
8 Y. Inokuma, S. Easwaramoorthi, Z. S. Yoon, D. Kim and A. Osuka, *J. Am. Chem. Soc.*, 2008, **130**, 12234.
9 Y. Inokuma, S. Easwaramoorthi, S. Y. Jang, K. S. Kim, D. Kim and A. Osuka, *Angew. Chem., Int. Ed.*, 2008, **47**, 4840.
10 J. Sung, P. Kim, S. Saga, S. Hayashi, A. Osuka and D. Kim, *Angew. Chem., Int. Ed.*, 2013, **52**, 12632.
11 E. Trurumaki, J. Sung, D. Kim and A. Osuka, Subporphyrinato boron(III) hydrides, *J. Am. Chem. Soc.*, 2015, **137**, 1056.
12 G. Copley, D. Hwang, K. Kim and A. Osuka, *Angew. Chem., Int. Ed.*, 2016, **55**, 10287.
13 W. J. Belcher, P. D. W. Boyd, P. J. Brothers, M. J. Liddle and C. E. F. Rickard, *J. Am. Chem. Soc.*, 1994, **116**, 8416.
14 P. J. Brothers, *Chem. Commun.*, 2008, 2090.
15 E. Tsurumaki, S. Hayashi, F. S. Tham, C. A. Reed and A. Osuka, *J. Am. Chem. Soc.*, 2011, **133**, 11956.
16 T. Kato, F. S. Tham, P. D. Boyd and C. A. Reed, *Heteroat. Chem.*, 2006, **17**, 209.
17 F. Zettler, H. D. Hausen and H. Hess, *Organomet. Chem.*, 1974, **72**, 157.
18 Z. Zhou, A. Wakamiya, T. Kushida and S. Yamaguchi, *J. Am. Chem. Soc.*, 2012, **134**, 4529.
19 S. Saito, K. Matsuo and S. Yamaguchi, *J. Am. Chem. Soc.*, 2012, **134**, 9130.
20 C. Dou, S. Saito, K. Matsuo, I. Hisaki and S. Yamaguchi, *Angew. Chem., Int. Ed.*, 2012, **51**, 12206.
21 T. Kushida, C. Camacho, A. Shuto, S. Irle, M. Muramatsu, T. Katayama, S. Ito, Y. Nagasawa, H. Miyasaka, E. Sakuda, N. Kitamura, Z. Zhou, A. Wakamiya and S. Yamaguchi, *Chem. Sci.*, 2014, **5**, 1296.
22 K. Matsuo, S. Saito and S. Yamaguchi, *J. Am. Chem. Soc.*, 2014, **136**, 12580.
23 K. Fuimoto, J. Oh, H. Yorimitsu, D. Kim and A. Osuka, *Angew. Chem., Int. Ed.*, 2016, **55**, 3196.
24 K. Berlin and E. Breitmaier, *Angew. Chem., Int. Ed.*, 1994, **33**, 1246.
25 M. Stępień and L. Latos-Grażyński, *Acc. Chem. Res.*, 2005, **38**, 88.

© 2025 The Author(s). Published by the Royal Society of Chemistry

Open Access Article. Published on 03 2024. Downloaded on 12.5.2026 15:04:04.
This article is licensed under a Creative Commons Attribution-NonCommercial 3.0 Unported Licence.

26 M. Stępień and L. Latos-Grażyński, *Chem.–Eur. J.*, 2001, **7**, 5113.
27 M. Stępień and L. Latos-Grażyński, *J. Am. Chem. Soc.*, 2002, **124**, 3838.
28 B. Szyszko, M. J. Bialek, E. Pacholska-Dudziak and L. Latos-Grażyński, *Chem. Rev.*, 2017, **117**, 2839.
29 T. D. Lash, S. T. Chaney and D. T. Richter, *J. Org. Chem.*, 1998, **63**, 9076.
30 T. D. Lash, *Org. Biomol. Chem.*, 2015, **13**, 7846.
31 T. D. Lash, *Chem. Rev.*, 2017, **117**, 2313.
32 R. Mysliborski, L. Latos-Grażyński, L. Szterenberg and T. Lis, *Angew. Chem., Int. Ed.*, 2006, **45**, 3670.
33 L. Liu, J. Kim, L. Xu, Y. Rao, M. Zhou, B. Yin, J. Oh, D. Kim, A. Osuka and J. Song, *Angew. Chem., Int. Ed.*, 2022, **61**, e202214342.
34 N. J. Bialek, K. Hurej, H. Furuta and L. Latos-Grażyński, *Chem. Soc. Rev.*, 2023, **52**, 2082.
35 M. Toganoh and H. Furuta, *Chem. Commun.*, 2012, **48**, 937.
36 Y. Hisamune, K. Nishimura, K. Isakari, M. Ishida, S. Mori, S. Karsawa, T. Kato, S. Lee, D. Kim and H. Furuta, *Angew. Chem., Int. Ed.*, 2015, **54**, 7323.
37 T. Tanaka and A. Osuka, *Chem. Rev.*, 2017, **117**, 2584.
38 F. Luo, L. Liu, H. Wu, L. Xu, Y. Rao, M. Zhou, A. Osuka and J. Song, *Nat. Commun.*, 2023, **14**, 5028.
39 T. D. Lash, L. M. Stateman and D. I. AbuSalim, *J. Org. Chem.*, 2019, **84**, 14733.
40 Z. Cen, C. S. Wannere, C. Corminboeuf, R. Puchta and P. v. R. Schleyer, *Chem. Rev.*, 2005, **105**, 3842.
41 D. W. Szczepanik, M. Andrzejak, K. Dyduch, E. Żak, M. Makowski, G. Mazur and J. Mrozek, *Phys. Chem. Chem. Phys.*, 2014, **16**, 20514.
42 D. W. Szczepanik, M. Andrzejak, J. Dominikowska, B. Pawełek, T. M. Krygowski, H. Szatylowicz and M. Solá, *Phys. Chem. Chem. Phys.*, 2017, **19**, 28970.
43 J. Y. Shin, K. S. Kim, M. C. Yoon, J. M. Lim, Z. S. Yoon and D. Kim, *Chem. Soc. Rev.*, 2010, **39**, 2751.
44 J. Oh, Y. M. Sung, Y. Hong and D. Kim, *Acc. Chem. Res.*, 2018, **51**, 1349.
45 J. Kim, J. Oh, A. Osuka and D. Kim, *Chem. Soc. Rev.*, 2022, **51**, 268.

© 2025 The Author(s). Published by the Royal Society of Chemistry